Research Article

Chemical Review and Letters
journal homepage: www.chemrevlett.com
ISSN (online): 2645-4947 (print) 2676-7279

Enhanced catalytic performance of Pt nanoparticles incorporated neodymium-cupper-iron mixed metal oxide nanoparticles on polyaniline-chitosan substrate as new catalyst for methanol electro-oxidation

Somaye Khammarnia[1,*], Mehri-Saddat Ekrami-Kakhki [2], Jilla Saffari[3]

[1]*Chemistry Department, Payame Noor University, 19395-4697, Tehran, Iran*
[2]*Department of Chemical Engineering, Esfarayen University of Technology, Esfarayen, North Khorasan, Iran*
[3]*Department of Chemistry, Zahedan Branch, Islamic Azad University, P.O. Box 98135-978, Zahedan, Iran*

ARTICLE INFO

Article history:
Received 12 April 2025
Received in revised form 17 May 2025
Accepted 18 May 2025
Available online 30 July 2025

Keywords:
Nanocatalyst
Chitosan
Polyaniline
Methanol electro-oxidation

ABSTRACT

In this research, $Nd_2CuFe_2O_7$ (NCuFO) nanoparticles were synthesized through the coprecipitation method and identified by energy dispersive X-ray (EDX), elemental distribution map, field emission scanning electron microscopy (FESEM), and transmission electron microscopy (TEM) analyses. Polyaniline (PANI) and chitosan (CHS) were used as effective and suitable substrates for nanoparticles. A novel Pt-NCuFO/PANI-CHS nanocatalyst was prepared by chemical reduction of hexachloroplatinic acid in the presence of NCuFO nanoparticles on the PANI-CHS substrate. The nanoparticles' distribution on the substrate was shown by TEM images. The catalytic performance of the Pt-NCuFO/PANI-CHS for methanol electro-oxidation was evaluated, compared to Pt/PANI-CHS. The effects of several experimental factors for methanol electro-oxidation were investigated. Pt-NCuFO/PANI-CHS catalyst showed better antipoisoning effect, higher electrochemically active surface area, and better stability towards methanol oxidation than Pt/PANI-CHS catalyst. The improved catalytic performance of Pt-NCuFO/PANI-CHS, compared to Pt/PANI-CHS suggests its promising application in direct methanol fuel cells.

1. Introduction

Today, the main focus of human civilization is the environment, alternative energy sources and information technology, as people around the world are trying to establish a relationship between the environment and modern life. [1]. Renewable, efficient, and environmentally friendly alternative energy sources, which are one of the main challenges in the world today, are under research and development. Fuel cells seem to be the potential answer to this challenge [2]. In the past decades, fuel cells have attracted much attention as energy converters with high efficiency, and low/zero emissions due to the high energy demand, reduction of fossil fuels, and reduction of environmental pollution. Direct methanol fuel cells (DMFCs) use methanol fuel, which is easy to transport and store, simplifying fuel cell systems. DMFCs have outstanding properties, including low operating temperature, easy fluid handling, as well as high energy density, which make them promising candidates for the power supply of portable electronic devices. Although many studies have been conducted in this field, DMFCs have several problems that need to be addressed in terms of efficiency as well as power density [3, 4]. Platinum (Pt) has a high electrocatalytic performance for methanol oxidation (MO) at low temperatures below 100 °C [5]. Since the early 1970s, researchers have thoroughly investigated the oxidation of methanol, in particular the identification of reaction intermediates, the modification of the platinum surface as well as the toxic species and products to achieve better resistance to poisoning and higher activity at lower potentials. Several authors have reviewed the results.

* Corresponding author; e-mail: somayekhammarnia@pnu.ac.ir
https://doi.org/10.22034/crl.2025.512011.1558

Although significant amounts of methyl formate, formic acid, and formaldehyde were detected, the main product of the reaction was CO_2. Further research shows that the most important reactions are methanol absorption and CO oxidation. Platinum is a very active metal for adsorbing methanol decomposers. However, CO can easily poison platinum at room or moderate temperatures [6]. Although DMFCs are proposed as promising energy sources due to their high conversion energy efficiency, their commercialization is hindered by obstacles such as the low kinetics of MO as well as the penetration of methanol into the proton exchange membrane. There is a general agreement that the key reason for the slow kinetics of MO is the CO species produced during MO. The most commonly accepted strategy for the prevention of CO poisoning is the use of platinum/metal oxide composites or platinum-based alloys according to the electronic effect and functional mechanism [7]. Beyond energy conversion applications, nanocatalysts in organic synthesis—leveraging nanoscale particle size, enlarged active surface area, and engineered metal–oxide/support interfaces—consistently deliver enhanced activity, selectivity, and resistance to deactivation [8, 9]. Likewise, polymer-based nanocomposites (e.g., PANI–CHS), readily synthesized via solution/gel routes, have been widely applied to dye and pollutant adsorption owing to their tunable porosity and abundant functional groups, underscoring the importance of interfacial engineering and dispersion control [10-19]. Guided by these principles, we uniformly disperse platinum nanoparticles on a conductive PANI-CHS matrix and couple them with the mixed-metal oxide $Nd_2CuFe_2O_7$ (NCuFO) to supply surface oxygen species and efficient charge-transport pathways, thereby enhancing methanol electro-oxidation kinetics, operational stability, and CO tolerance. Various metal oxides such as Pr, Sm, and Ce in mesoporous carbon have been used to increase the performance of Pt nanoparticles for methanol oxidation reaction (MOR) [20]. In recent years, perovskites with chemical composition $ABO_{3-\delta}$ and with outstanding electrical conductivity are considered promising candidates for the direct methanol fuel cell's anode [21, 22]. The uniform dispersion of platinum nanoparticles in a suitable polymer substrate or the platinum nanoparticles' deposition on cheap metal materials is one of the ways to increase the catalytic activity of platinum for the oxidation of alcohols and reduce the cost of anode materials in the fuel cells' applications [23-26]. Good environmental resistance, cheap production in large quantities, easy control, and easy synthesis are the properties that make polyaniline (PANI) commercially attractive. PANI has been widely investigated for its electrochemical, chemical, optical, and electrical properties. In addition, it is resistant to air and has an easy synthesis method. However, the impenetrability and solubility in common organic solvents are the main disadvantages of PANI [27]. This material is easily used as foam. The thin film is not made with good mechanical properties, so its application is limited in practice. In this regard, many efforts have been made to make polyaniline composites with better processability, and mechanical properties while maintaining the conductivity of the polymer. Recently, mixtures containing conductive polymer and hydrogel have attracted considerable attention, because they can produce electroactive hydrogels capable of physical or chemical transport in response to the electrical potentials. Chitosan (CHS) as a copolymer of 2-acetamide-2-deoxy-D-glucopyranose and 2-amino-2-deoxy-D-glucopyranose using glutaraldehyde cross-linking agents has a crosslinked styrene polymer with hydrogel-like properties. CHS in the form of hydrogel has many applications such as separation membranes, wastewater treatment, food packaging, wound healing, and drug delivery systems [28]. In this research work, after the preparation of NCuFO nanoparticles, the novel Pt-NCuFO/PANI-CHS nanocomposite was synthesized by chemical reduction of hexachloroplatinic acid in the presence of NCuFO nanoparticles on PANI-CHS substrates. The performance of the Pt-NCuFO/PANI-CHS nanocomposite for methanol oxidation was investigated for the first time, and compared with that of Pt/PANI-CHS. The electrochemical investigations were performed through different electrochemical techniques, including cyclic voltammetry (CV), chronoamperometry (CA), and electrochemical impedance spectroscopy (EIS). The results showed that the catalytic performance of Pt-NCuFO/PANI-CHS nanocatalyst for MOR was much better than that of Pt/PANI-CHS nanocatalyst.

2 Materials and methods

Fe $(NO_3).9H_2O$, $NdCl_3.6H_2O$ (98%), $CuCl_2.6H_2O$, NaOH, and octanoic acid from Merck were used for the synthesis of NCuFO nanocatalyst. Hexachloroplatinic acid and sodium tetrahydroborate from Merck were used to prepare the platinum nanoparticles. Polyaniline was obtained from Sigma Aldrich. Chitosan was purchased from Fluka and used as a substrate for the preparation of Pt-NCuFO/PANI-CHS nanocatalyst. Sulfuric acid (98% Merck) was used as electrolyte. 1% acetic acid solution (refrigerated, 100% Merck) was used to prepare the CHS solution. Methanol (99.2%) was purchased from Merck and its oxidation was investigated. A potentiostat/galvanostat Autolab apparatus (model PGSTAT 302N, Metrohm, Netherlands) was used to perform the electrochemical studies. A three-electrode cell was applied. A saturated calomel (SCE) electrode, a glassy

carbon (GC) electrode, and a platinum electrode were used as reference, working, and counter electrodes, respectively.

2.1 Preparation of nanocatalyst

To prepare the NCuFO nanocatalyst, first 0.0111 mol of $NdCl_3.6H_2O$, 0.11 mol of $Fe(NO_3)_3.9H_2O$, and 0.0055 mol of $CuCl_2.6H_2O$ were each dissolved in 10 mL of distilled water and mixed. Next, 2 ml of octanoic acid was poured into the solution and stirred vigorously. The solution pH was adjusted to 9 using 5 M NaOH. The precipitate was washed and dried. Afterwards, the powder was calcined at 800°C for 4 hours. NCuFO nanocatalyst was synthesized and identified.

2.2 Synthesis of Pt-NCuFO/PANI-CHS nanocomposite

To prepare the Pt-NCuFO/PANI-CHS nanocatalyst, first, 1 mg of PANI was dissolved in a mixture of CHS and deionized water (1:7 ratio). After adding 2 mg of NCuFO catalyst, sonication was performed for 1 hour. Then, 25 µl of hexachloroplatinic acid 1 M was added to the solution and stirred for one hour. Later, 50 µl of sodium tetrahydroborate 5 M was added to the mixture. After stirring for 24 hours, the resulting mixture was centrifuged and washed several times with deionized water. Pt-NCuFO/PANI-CHS nanocatalyst was prepared after drying the mixture for 12 hours at 60°C. Pt/PANI-CHS nanocatalyst was prepared using the same method without using NCuFO nanoparticles.

2.3. Preparation of electrodes

In order to prepare the GC/Pt/PANI-CHS and GC/Pt-NCuFO/PANI-CHS modified electrodes, 2 mg of the catalyst powder was added to 1 ml of CHS solution and sonicated for ten minutes. Then 5 µl of the respective suspension was placed on the surface of glassy carbon electrodes and dried at room temperature.

3. Results and discussion

3.1. Characterization of the catalysts

The elemental distribution map of the NCuFO nanoparticles is shown in Fig. 1A. EDX analysis also confirms the formation of NCuFO trimetallic mixed oxide nanocatalyst (Fig. 1B). The elemental composition of the catalyst is presented in the inset of Fig. 1B. The morphology and size distribution of the particles have been investigated from the TEM images. The TEM image of NCuFO nanocatalyst is shown in Fig. 1C. The synthesized nanoparticles have a spherical shape with a mean particle size of 13.75 nm, which is in good agreement with the XRD results. The formation of NCuFO nanocatalyst was identified by FESEM analysis, indicated in Fig. 1D. As shown, the NCuFO nanocatalyst has a porous structure. This porous structure forms many active sites on the surface which can be a good host for guest ions. TEM images of Pt/PANI-CHS and Pt-NCuFO/PANI-CHS nanocatalysts are exhibited in Fig. 2. As shown, the spherical Pt nanoparticles are distributed in the PANI-CHS matrix and around the NCuFO nanoparticles. The average particle size of Pt and NCuFO nanoparticles was approximately 3.58 nm and 13.41 nm, respectively.

3.2. Electrocatalytic studies

Fig. 3A shows the electrochemical behavior of Pt/PANI-CHS and Pt-NCuFO/PANI-CHS in sulfuric acid 0.5 M. The electrochemical active surface (EAS) was obtained by measuring hydrogen adsorption and desorption charges in 0.5 M sulfuric acid using equation (1) [29].

$$EAS = {Q_H}/{0.21 \times [Pt]} \quad (1)$$

In this equation, Q_H represents the columbic charge for hydrogen absorption and desorption, and 0.21 mC cm^{-2} is the required charge to absorb hydrogen monolayers on the surface of platinum nanoparticles. The platinum loading [Pt] on the GC electrode was 2.056 µg, obtained by inductively coupled plasma optical emission spectroscopy [30].

With the uniform loading of Pt nanoparticles, the electrochemical active surface area value for the Pt-NCuFO/PANI-CHS catalyst (160.58 m^2g^{-1}) was much higher than that of Pt/PANI-CHS (54.69 m^2g^{-1}), indicating its higher catalytic performance and higher amounts of active sites for MO than Pt/PANI-CHS [31] (Fig. 3B). Thus, Pt-NCuFO/PANI-CHS is expected to have the enhanced electrocatalytic activity for MOR, compared to Pt/PANI-CHS.

The catalytic performance of Pt/PANI-CHS and Pt-NCuFO/PANI-CHS nanocatalysts for methanol electro-oxidation was studied in sulfuric acid 0.5 M and methanol 1.5 M (Fig. 3c). The synthesized catalysts had two oxidation peaks for methanol electro-oxidation. The first anodic peak (j_f) in the forward scan is related to the electro-oxidation of methanol and the second oxidation peak (j_b) is related to the oxidation of intermediates produced during MO [32]. In Pt-NCuFO/PANI-CHS and Pt/PANI-CHS nanocatalysts, the first MO peak was observed at 0.861 and 0.763 V, respectively. The second MO peak was observed in the reverse scan at 0.594 and 0.463 V, respectively. As shown in Fig 3D, Pt-NCuFO/PANI-CHS had enhanced electrocatalytic activity, compared to Pt/PANI-CHS catalyst.

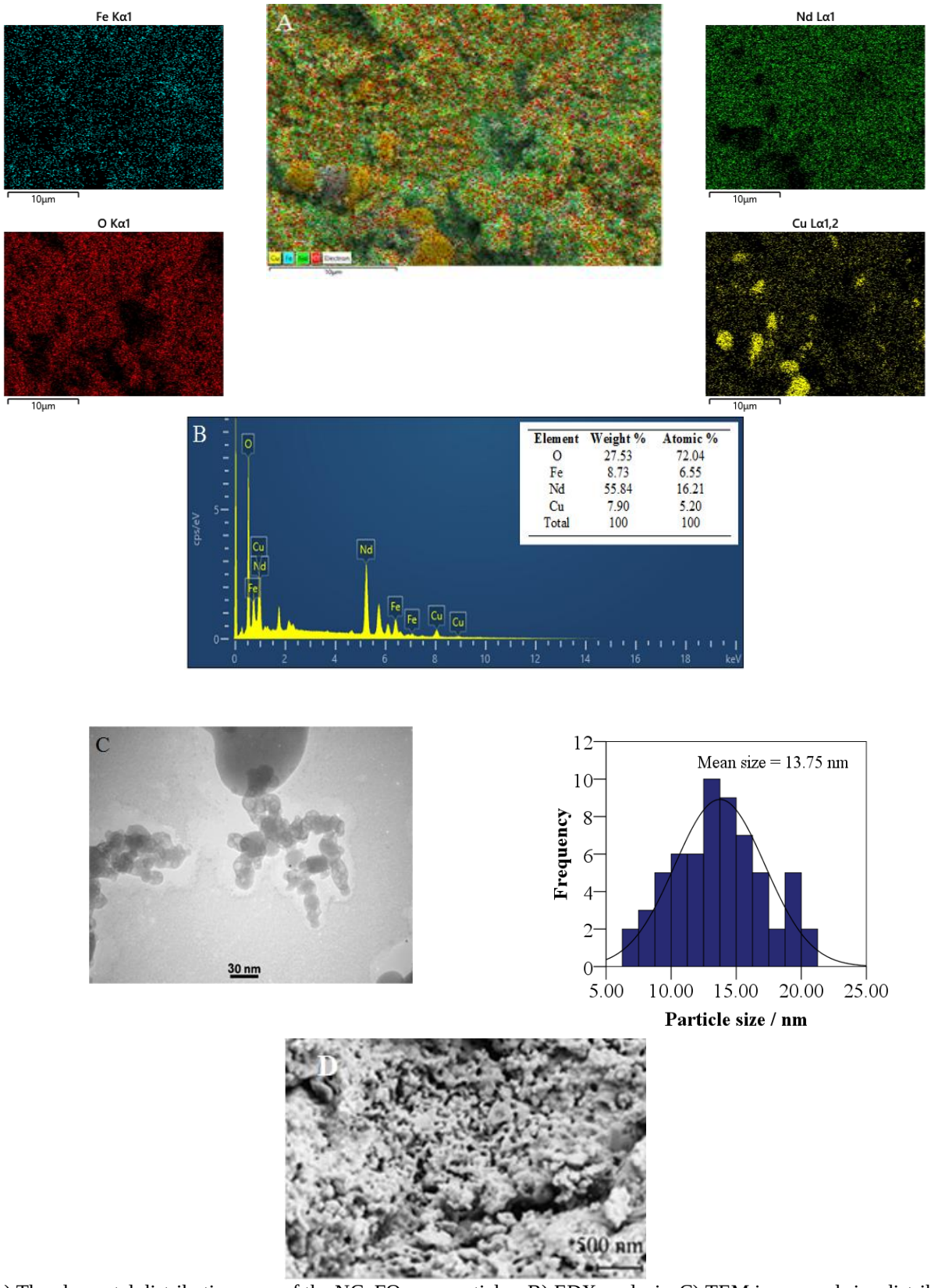

Fig. 1. A) The elemental distribution map of the NCuFO nanoparticles, B) EDX analysis, C) TEM image and size distribution of NCuFO nanoparticles and C) FESEM image

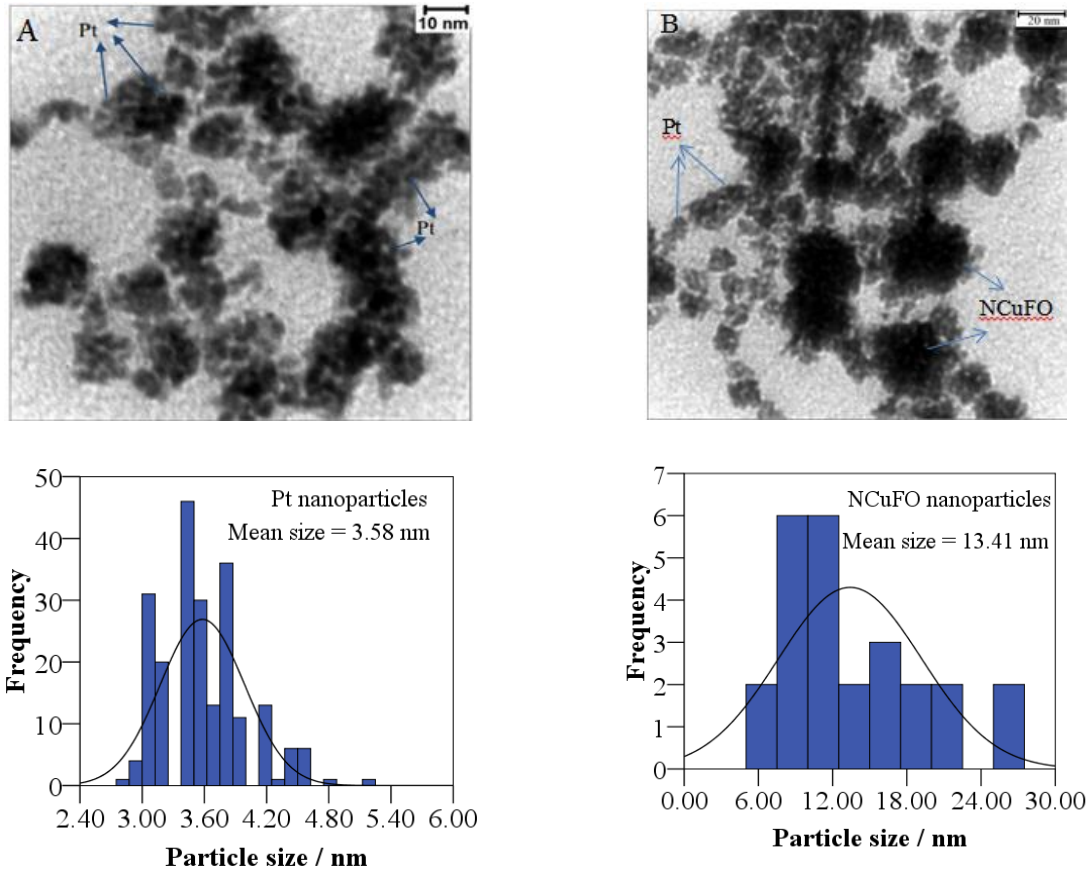

Fig. 2. TEM images of A) Pt/PANI-CHS and B) Pt-NCuFO/PANI-CHS catalysts. Histograms of particle size distribution are also shown.

The mass activity of the anodic peak of MO at Pt-NCuFO/PANI-CHS (11397.073 mA mg^{-1}_{Pt}) was higher than that of Pt/PANI-CHS (6120.488 mA mg^{-1}_{Pt}). Pt-NCuFO/PANI-CHS exhibited enhanced catalytic activities for MOR in comparison with Pt/PANI-CHS. The incorporation of NCuFO with PANI-CHS and their use with Pt nanoparticles improved the Pt catalytic performance for MOR. The behavior of Pt/PANI-CHS and Pt-NCuFO/PANI-CHS for methanol electro-oxidation was investigated by electrochemical impedance spectroscopy (EIS). EIS analyses were carried out using Nyquist curves [33] in the range of 1×10^{-3} to 1×10^{-2} Hz at open circuit potential in 0.5 M sulfuric acid and 1.5 M methanol (Fig. 4A). The presence of a small semicircle in the high-frequency region in each Nyquist curve is attributed to the charge transfer process at the electrode and electrolyte interface. A straight line in the low-frequency region refers to the diffusion process in the synthesized catalysts. As shown in Fig. 4A, the Pt-NCuFO/PANI-CHS catalyst has a smaller semicircle diameter and a more vertical straight line than Pt/PANI-CHS indicating the faster kinetics of Pt-NCuFO/PANI-CHS for the ion diffusion process and the faster charge transfer reaction of this catalyst, compared to Pt/PANI-CHS for methanol electro-oxidation [34]. The chronoamperometry (CA) method was employed to measure the long-term stability of Pt-NCuFO/PANI-CHS and Pt/PANI-CHS catalysts for the MO reaction. CA curves were obtained at 0.8 V vs. SCE for 1000 s in 1.5 M methanol and 0.5 M H_2SO_4. As shown in Fig. 4B, the CA of Pt-NCuFO/PANI-CHS was better for methanol electro-oxidation compared to the Pt/PANI-CHS. Initially, the flux of the prepared catalysts decreased rapidly, which was probably due to the poisoning of the catalysts by the intermediates produced during MO [27]. First, the anodic current density (ACD) of Pt-NCuFO/PANI-CHS (416.59 mA cm^{-2}) was higher than Pt/PANI-CHS (202.59 mA cm^{-2}). After the measured time (1000 seconds), the anodic current density of Pt-NCuFO/PANI-CHS (100.49 mA cm^{-2}) was still higher than that of Pt/PANI-CHS (13.96 mA cm^{-2}). The Pt-NCuFO/PANI-CHS catalyst had higher initial current density and lower current density loss after 1000 s, compared to Pt/PANI-CHS (Fig. 4c). Pt-

NCuFO/PANI-CHS showed higher tolerance to the intermediates produced (such as CO) during MO [35], better stability and catalytic performance for methanol electro-oxidation, compared to the Pt/PANI-CHS catalysts. The electrochemical data of MOR at different catalysts are shown in Table 1 [36-44].

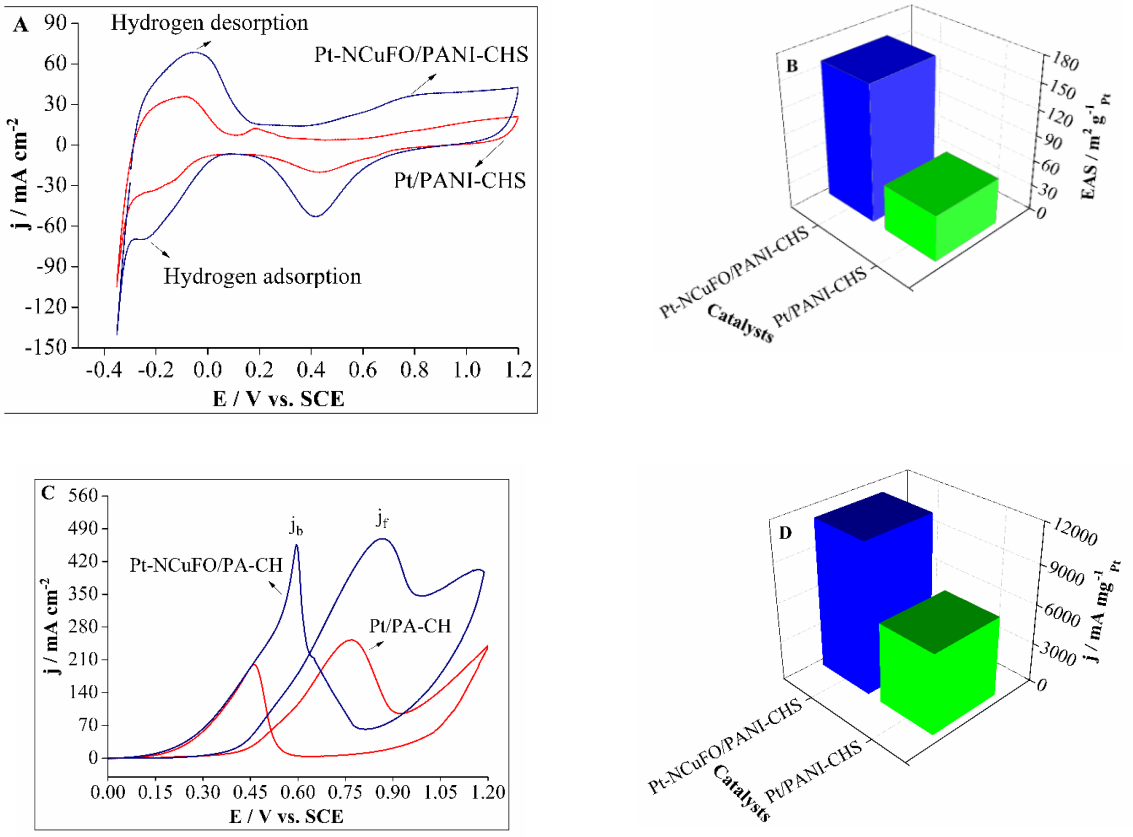

Fig. 3. A) CV curves and B) EAS plots of the catalysts in 0.5 M sulfuric acid. C) CV curves and D) Anodic peak mass activity plot of the synthesized catalysts in sulfuric acid 0.5 M and methanol 1.5 M.

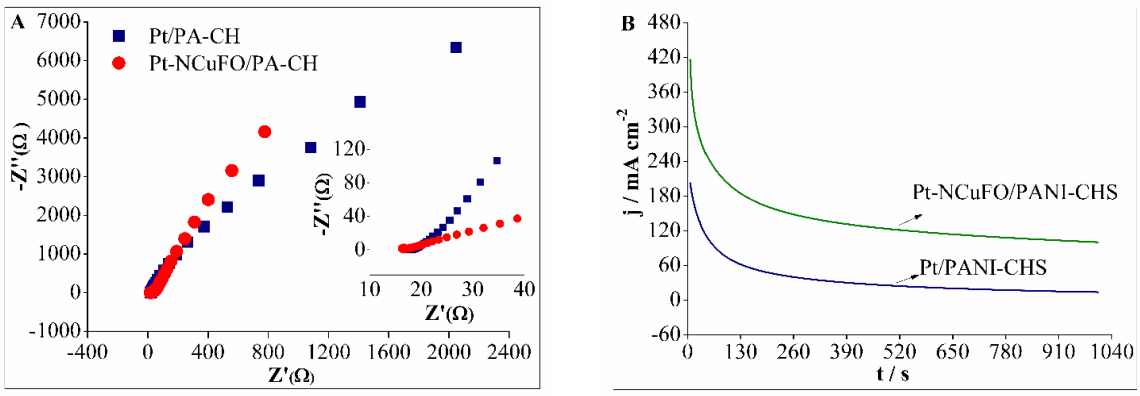

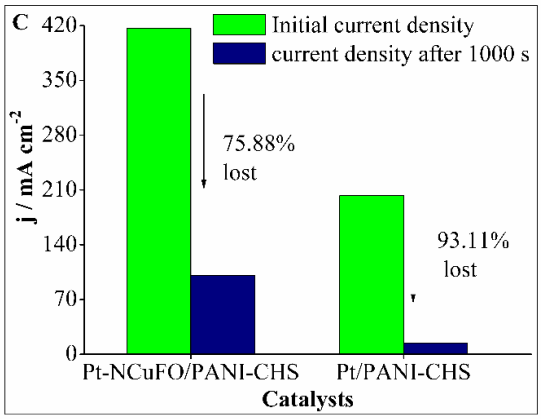

Fig 4. A) Nyquist curves and B) chronoamperometry curves of the catalysts in sulfuric acid 0.5 M and methanol 1.5 M and C) the initial and retained current density and activity decline ratio of the catalysts after 1000 s.

Table 1. The electrochemical data of methanol electrooxidation at different catalysts.

Catalysts	EAS ($m^2\ g^{-1}_{Pt}$)	E_f (V) vs. SCE	j_f mA mg^{-1}_{Pt})	ref
Pt-LFO/PA-CH	77.46	0.793	9209.268	[29]
Pt/PA-CH	54.69	0.766	4967.561	[29]
Pt/PVA-CuO-Co_3O_4/CH	54.56	0.810	3010.86	[30]
Pt/PVA-CuO-Co_3O_4	35.89	0.744	1597.984	[30]
Pt/OMCS	73.5	0.9 vs. NHE	510	[31]
Pt-$FeNi_2P$/C	90.47	0.641	1125	[32]
Pt/C-Au@CeO_2-Pt	77.8	0.8	1267	[33]
Commercial Pt/C	45.6	0.7	616	[33]
Commercial Pt/C (20% Pt)	65.7	0.65	258.5	[34]
Pt NPs/C	22	0.65	153.8	[35]
Pt NWs/NL-CNS	115.9	0.7	1949.5	[35]
Pt/C (C:Vulcan carbon)	39.67	0.62	192.97	[36]
Pt/PANI-CHS	54.69	0.763	6120.488	This work
Pt-NCuFO/PANI-CHS	160.58	0.861	11397.073	This work

4. Conclusions

In this study, Pt-NCuFO/PANI-CHS nanocatalysts were successfully synthesized by dispersing NCuFO and platinum nanoparticles on polyaniline and chitosan substrates. The electrocatalytic performance of the catalysts was determined for MOR and compared with that of Pt/PANI-CHS nanocatalyst. Pt-NCuFO/PANI-CHS showed excellent catalytic performance for MOR. It was shown that the presence of NCuFO nanoparticles along with Pt significantly increased its electrocatalytic performance for MOR. The Pt-NCuFO/PANI-CHS nanocatalyst had a higher electrochemically active surface area, higher anodic peak current density, higher anodic peak mass activity, and less poisoning effect, compared to Pt/PANI-CHS, indicating that Pt-NCuFO/PANI-CHS is a suitable catalyst for use in DMFCs.

References

[1] N.S. Ferreira, L.P.T. Carneiro, C. Viezzer, M.J.T. Almeida, A.C. Marques, A.M.F.R. Pinto, E. Fortunato, M.G.F. Sales, Passive direct methanol fuel cells acting as fully

autonomous electrochemical biosensors: Application to sarcosine detection. J. Electroanal. Chem., 922(2022) 116710.

[2] O.Z. Sharaf, M.F. Orhan, An overview of fuel cell technology: Fundamentals and applications. Renew. Sustain. Energy Rev., 32 (2014) 810-850.

[3] (a) M.S. Abdel-wahab, H.K. El Emam, W.M.A. El Rouby, Sputtered Ag-doped NiO thin films: structural, optical, and electrocatalytic activity toward methanol oxidation. J. Mater. Sci.: Mater. Electron., 34(2023) 1637; (b) C.L. Vecchio, D. Sebastián, C. Alegre, A.S. Aricò, V. Baglio, Carbon-supported Pd and Pd-Co cathode catalysts for direct methanol fuel cells (DMFCs) operating with high methanol concentration. J. Electroanal. Chem., 808(2018) 464-473; (c) E.E. Abdel-Hady, M. Shaban, M.O. Abdel-Hamed, A. Gamal, H. Yehia, A. M. Ahmed, Synthesis and Characterization of NiCoPt/CNFs Nanoparticles as an Effective Electrocatalyst for Energy Applications. J. Nanomater., 12(2022) 492.

[4] (a) R.Y. Hwang, Y.S. Byun, O.H. Han, Electrochemical phenomena in direct methanol fuel cells investigated by multiple NMR analyses of cathode and anode exhausts. J. Electroanal. Chem., 775(2016) 320-324; (b) V. Ramesh, B. Krishnamurthy, Modeling the transient temperature distribution in a direct methanol fuel cell. J. Electroanal. Chem., 809(2018) 1-7; (c) M.R. Shivhare, R.G. Allen, K. Scott, A.J. Morris, E.B. Martin, A kinetic model for the direct methanol fuel cell anode based on surface coverage. J. Electroanal. Chem., 595(2006) 145 -151.

[5] S.E. Herrera, M. Tagliazucchi, F.J. Williams, E.J. Calvo, Pt Nanoparticles in Polyelectrolyte Multilayers: Polymer Effects on the Electrocatalytic Activity for Methanol Oxidation . J. Electroanal. Chem., 938(2020) 117430.

[6] Q. Wang, S. Liu, S. An, X. Song, X. Liang, Z. Wang, Y. Mu, Platinum nanoparticles assembled on different carbon materials and flower-like CeO_2 for methanol electro-oxidation. J. Mater. Sci.: Mater. Electron., 32(2021) 26425-26438.

[7] J. Wang, J. Xi, Y. Bai, Y. Shen, J. Sunc, L. Chen, W. Zhu, X. Qiu, Short communication Structural designing of Pt-CeO2/CNTs for methanol electro-oxidation. J. Power Sources, 164(2007) 555–560.

[8] (a) S. Soleimani-Amiri, Z. Hossaini, Z. Azizi, Synthesis and Investigation of Biological Activity of New Oxazinoazepines: Application of Fe_3O_4/CuO/ZnO@MWCNT Magnetic Nanocomposite in Reduction of 4-Nitrophenol in Water. Polycycl. Aromat. Comp., 43(4) (2023) 2938-2959. https://doi.org/10.1080/10406638.2022.2058969; (b) E. Hemmati, S.h Soleimani-Amiri, M. Kurdtabar, A CMC-g-poly(AA-co-AMPS)/Fe_3O_4 hydrogel-nanocomposite as a novel biopolymer-based catalyst in the synthesis of 1,4-dihydropyridines. RSC Adv., 13(24) (2023) 16567-16583. https://doi.org/10.1039/D3RA01389H; (c) S. Soleimani Amiri, M. Ghazvini, S. Khandan, S. Afrashteh, KF/Clinoptilolite@MWCNTs Nanocomposites Promoted a Novel Four-Component Reaction of Isocyanides for the Green Synthesis of Pyrimidoisoquinolines in Water. Polycycl. Aromat. Comp., 42(7) (2022) 4736-4751. https://doi.org/10.1080/10406638.2021.1912122.

[9] (a) J. Wang, P. Su, S. Abdolmohammadi, E. Vessally, A walk around the application of nanocatalysts for cross-dehydrogenative coupling of C–H bonds, RSC adv., 9(71) (2019) 41684-41702. https://doi.org/10.1039/C9RA08752D; (b) S. Soleimani Amiri, Z. Hossaini, Z. Azizi, Synthesis and investigation of antioxidant and antimicrobial activity of new pyrazinopyrroloazepine derivatives using Fe_3O_4/CuO/ZnO@MWCNT MNCs as organometallic nanocatalyst by new MCRs. Appl. Organomet. Chem., 36(4) (2022) e6573. https://doi.org/10.1002/aoc.6573 (c) ; S. Soleimani Amiri, Y. Salemi, Novel butane sulfonic acid-functionalized core–shell magnetic nanocatalysts for ultrasound-assisted coumarin synthesis. New J. Chem., 48 (2024) 2299-2310. https://doi.org/10.1039/D3NJ04912D.

[10] S. Sallau, H. O. Enedubi, Improved optical properties of waste polystyrene nanocomposites with zinc oxide nanoparticles, reduced grapheme oxide, and kaolin fillers. J. Med. Nanomater. Chem., 7(3) (2025) 332–348;

[11] P. Badr, M. Sajjadnejad, S. M. S. Haghshenas, Influence of incorporating B_4C nanoparticles and pulse electrodeposition parameters on the surface morphology and wear behavior of nickel based nanocomposite coatings. Prog. Chem. Biochem. Res., 6(4) (2023) 292–313;

[12] L. Sohrabi-Kashani, A. Zolriasatein, B. Eftekhari Yekta, Effect of silica nanoparticles modified with different concentrations of stearic acid on microstructure, mechanical & electrical properties of RTV-2 silicone rubber nanocomposite. J. Med. Nanomater. Chem., 5(1) (2023) 16–32;

[13] H. Pourfaraj, S. Rostamzadeh Mansour, M. Zaefizadeh, A. Vojood, Synthesis and Characterization of Cisplatin Magnetic Nanocomposite. J. Med. Nanomater. Chem., 5(1) (2023) 92–105;

[14] F. Ali, S. Fazal, N. Iqbal, A. Zia, F. Ahmad, PANI-based nanocomposites for the removal of dye from wastewater. J. Med. Nanomater. Chem., 5(2) (2023) 106–124.

[15] A. Heidaripour, H. Gholami Qasemi, Innovative preparation of Mica/Fe_3O_4 superparamagnetic nanocomposite as a contrast agent in MRI and MHT. J. Med. Nanomater. Chem., 5(2) (2023) 125–134;

[16] A. Belhachem, N. Amara, H. Belmekki, Y. Yahia, Z. Cherifi, A. Amiar, A. Bengueddach, R. Meghabar, H. Toumi, Synthesis, characterization and anti-inflammatory activity of an alginate–zinc oxide nanocomposite. J. Med. Nanomater. Chem., 5(3) (2023) 173–185;

[17] A. Heidaripour, H. Panahi, G. Attari, F. Jahansooz, Fabrication of nanocomposite of HAp-SiO_2-Fe_3O_4 suitable for magnetic hyperthermia. J. Med. Nanomater. Chem., 6(4) (2024) 251–262;

[18] G. Kouchakzadeh, N. Derikvand, A. Khorramabadi,, Synthesis and assessment of polyaniline-intercalated Zn-Al layered double hydroxides nanocomposites as an approach for improvement of conductivity property. J. Med. Nanomater. Chem., 7(1) (2025) 84–97;

[19] I. J. Radhi, S. A. Hassan, A. F. Alkaim, Preparation and characterization of ZnO, WO_3/ZnO nanocomposites using hydrothermal method. J. Nanostruct., 13 (2023) 1133-1141.

[20] S.J. Zaidi, M. Bello, A. Al-Ahmed, A.B. Yousaf, M. Imran, Mesoporous carbon supported Pt/MO_2 (M = Ce, Pr, Nd, Sm) heteronanostructure: Promising non-Ru methanol oxidation reaction catalysts for direct methanol fuel cell application. J. Electroanal. Chem., 794 (2017). 86-92.

[21] Z. Yavari, M. Noroozifar, T. Parvizi, Performance evaluation of anodic nano-catalyst for direct methanol alkaline fuel cell. Environ. Prog. Sustain., 37(2018) 597-604.

[22] H.C. Yu, K.Z. Fung, T.C. Guo, W.L. Chang, Syntheses of perovskite oxides nanoparticles La1−xSrxMO3− (M = Co and Cu) as anode electrocatalyst for direct methanol fuel cell. Electrochim. Acta, 50(2004) 811–816.

[23] Z. Merati, J. Basiri Parsa, R. Babaei-Sati, Electrochemically synthesized polypyrrole/MWCNTs-Al2O3 ternary nanocomposites supported Pt nanoparticles toward methanol oxidation. Int. J. Hydrogen Energy, 43(2018) 20993-21005.

[24] J. Azizi, M.A. Kamyabi, Pulse-electrodeposition of PtNi nanoparticles on a novel substrate of multi-walled carbon nanotubes/poly(eriochrome blue-black B) as an active and durable catalyst for the electrocatalytic oxidation of methanol. J. Electroanal. Chem., 920(2022) 116642.

[25] G. Foti, C. Mousty, K. Novy, C. Comninellis, V. Reid, Pt/Ti electrode preparation methods: application to the electrooxidation of isopropanol. J. Appl. Electrochem., 30(2000) 147-151.

[26] R. Yan, B. Jin, D. Li, One-step electrochemically co-deposited Pt nanoparticles/polyaniline composites with raspberry structures for methanol electro-oxidation. Synth. Met., 235(2018) 110 -114.

[27] A.G. Yavuz, A. Uygun, V.R. Bhethanabotla, Preparation of substituted polyaniline/chitosan composites by *in situ* electropolymerization and their application to glucose sensing. Carbohy. Poly., 81(2010) 712- 719.

[28] T. Thanpitcha, A. Sirivat, A.M. Jamieson, R. Rujiravanit, Preparation and characterization of polyaniline/chitosan blend film. Carbohy. Poly., 64(2006) 560 -568.

[29] K. Kakaei, A. Rahimi, S. Husseindoost, M. Hamidi, H. Javan, A. Balavandi, Fabrication of Pt-CeO2 nanoparticles supported sulfonated reduced graphene oxide as an efficient electrocatalyst for ethanol oxidation. Int. J. Hydrogen Energy, 41(2016) 3861-3869

[30] M.S. Ekrami-Kakhki, N. Farzaneh, S. Abbasi, B. Makiabadi, Electrocatalytic activity of Pt nanoparticles supported on novel functionalized reduced graphene oxide-chitosan for methanol electrooxidation. J. Mater. Sci.: Mater. Electron., 28(2017) 12373-12382.

[31] F. Xie, M. Gan, M. Jiang, L. Ma, Fe-doped CoP nanotube heterostructure enhanced the catalytic activity of Pt nanoparticles towards methanol oxidation reaction. Int. J. Hydrogen Energy, 45(2020) 24807 -24817.

[32] M. Noroozifar, M. Khorasani-Motlagh, R. Khaleghian-Moghadam, M.S. Ekrami-Kakhki, M. Shahraki, Incorporation effect of nanosized perovskite $LaFe_{0.7}Co_{0.3}O_3$ on the electrochemical activity of Pt nanoparticles-multi walled carbon nanotube composite toward methanol oxidation. J. Solid State Chem., 201(2013) 41 -47.

[33] K. Ding, Z. Jia, Q. Wang, X. He, N. Tian, R. Tong, X. Wang, Electrochemical behavior of the self-assembled membrane formed by calmodulin (CaM) on a Au substrate. J. Electroanal. Chem., 513(2001) 67- 71.

[34] Q. He, W. Chen, S. Mukerjee, S. Chen, F. Laufek, Carbon-supported PdM (M = Au and Sn) nanocatalysts for the electrooxidation of ethanol in high pH media. J. Power Sources, 18(2009) 298-304.

[35] F. Zhang, Z. Wang, K.Q. Xu, J. Xia, Q. Liu, Z. Wang, Highly dispersed ultrafine Pt nanoparticles on nickel-cobalt layered double hydroxide nanoarray for enhanced electrocatalytic methanol oxidation. Int. J. Hydrogen Energy, 43(2018) 16302 -16310.

[36] XT. Li, H. Lei, C. Yang, Q.B. Zhang, Electrochemical fabrication of ultra-low loading Pt decorated porous nickel frameworks as efficient catalysts for methanol electrooxidation in alkaline medium. J. Power Sources, 396(2018) 64-72.

[37] S. Khammarnia, J. Saffari, M.-S. Ekrami-Kakhki, A. Akbari, Synthesis and study of highly effective catalytic activity of platinum-orthoferrite nanoparticlesLanthanum placed in polyaniline-chitosan substrate for electrooxidation Methanol. Adv. Processes Mater. Eng., 13(2019) 43-55.

[38] M.S. Ekrami-Kakhki, A. Naeimi, F. Donyagard, Pt nanoparticles supported on a novel electrospun polyvinyl alcohol-CuO-Co_3O_4/chitosan based on Sesbania sesban plant as an electrocatalyst for direct methanol fuel cells. Int. J. Hydrogen Energy, 44(2019) 1671 -1685.

[39] C.W. Zhang, L.B. Xu, J.F. Chen, High loading Pt nanoparticles on ordered mesoporous carbon sphere arrays for highly active methanol electro-oxidation. Chin. Chem. Lett., 27(2016) 832 -836.

[40] D. Wei, L. Ma, M. Gan, S. Han, J. Shen, J. Ding, W. Zhan, C. Zhou, X. Zhong, F. Xie, Pt-based catalyst decorated by bimetallic $FeNi_2P$ with outstanding CO tolerance and catalytic activity for methanol electrooxidation. Int. J. Hydrogen Energy, 45(2020) 4875-4886.

[41] D.V. Dao, G. Adilbish, T.D. Le, T.T.D. Nguyen, I.H. Lee, Y.T. Yu, Au@CeO_2 nanoparticles supported Pt/C electrocatalyst to improve the removal of CO in methanol oxidation reaction. J. Catal., 377(2019) 589-599.

[42] J.P. Zhong, C. Hou, L. Li, M. Waqas, Y.J. Fan, X.C. Shen, W. Chen, L.Y. Wan, H.G. Liao, S.G. Sun, A novel strategy for synthesizing Fe, N, and S tridoped graphene-supported Pt nanodendrites toward highly efficient methanol oxidation. J. Catal., 381(2020) 275-284.

[43] H. Huang, Y. Wei, Y. Yang, M. Yan, H. He, Q. Jiang, X. Yang, J. Zhu, Controllable synthesis of grain boundary-enriched Pt nanoworms decorated on graphitic carbon nanosheets for ultrahigh methanol oxidation catalytic activity. J. Energy Chem., 57(2021) 601-609.

[44] J. Chang, L. Feng, C. Liu, W. Xing, X. Hu, Ni_2P enhances the activity and durability of the Pt anode catalyst in direct methanol fuel cells. Energy Environ. Sci., 7(2014) 1628-1632.